ORGANIC LETTERS

2008
Vol. 10, No. 19
4191−4194

Structure of Membrane-Bound Amphidinol 3 in Isotropic Small Bicelles

Toshihiro Houdai, Nobuaki Matsumori,* and Michio Murata*

Department of Chemistry, Graduate School of Science, Osaka University, 1-1 Toyonaka, Osaka 560- 0043, Japan

matsmori@chem.sci.osaka-u.ac.jp; murata@ch.wani.osaka-u.ac.jp

Received July 17, 2008

ABSTRACT

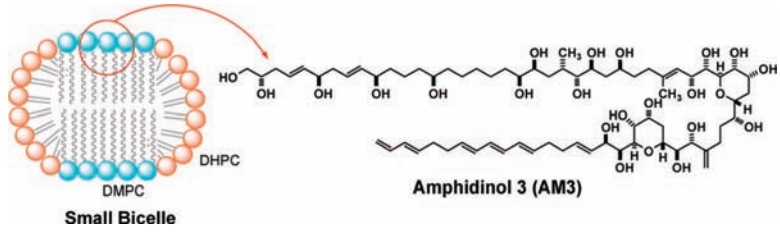

Amphidinol 3 (AM3) exhibits a potent membrane permeabilizing activity by forming pores in biological membranes. We examined the conformation and location of AM3 using isotropic bicelles, a more natural membrane model than micelles. The results show that AM3 takes turn structures at the two tetrahydropyran rings. Most of the hydrophilic region of the molecule is predominantly present in the surface, while the hydrophobic polyolefin penetrates in the bicelle interior.

Amphidinols (AMs) have been isolated as potent antifungal agents from the dinoflagellate *Amphidinium klebsii*. Several congeners including those bearing closely related structures with different names have been so far reported.[1−10] Among those, amphidinol 3 (AM3), whose absolute configuration was determined by our group,[7] has the most potent antifungal and hemolytic activities. Their structures are characterized by long carbon chains encompassing multiple hydroxyl groups and polyolefins, which endow amphiphilic nature to the molecules. AMs enhance the permeability of the biological membrane by direct interaction with the membrane lipids, which is thought to be responsible for their potent antifungal activity.[3,4,11−13] Our previous studies showed that in the presence of sterol AMs induce the membrane permeabilization by forming pores or lesions in phospholipid bilayers.[3,4,11−13] The size of the pore/lesion formed in the erythrocyte membrane was estimated to be 2.0−2.9 nm in diameter.[12] More recently, we have examined structure−activity relations using naturally occurring AMs and chemically modified AM derivatives with structural variations in polyhydroxy and polyene moieties[7] and found that the polyene and polyhydroxy moieties play roles in binding to the lipid bilayer membrane and in forming an ion-permeable pore/lesion across the membrane, respectively. Besides, to gain

(1) Satake, M.; Murata, M.; Yasumoto, T.; Fujita, T.; Naoki, H. *J. Am. Chem. Soc.* **1991**, *113*, 9859–9861.
(2) Paul, G. K.; Matsumori, N.; Murata, M.; Tachibana, K. *Tetrahedron Lett.* **1995**, *36*, 6279–6283.
(3) Paul, G. K.; Matsumori, N.; Konoki, K.; Sasaki, M.; Murata, M.; Tachibana, K. In *Harmful and Toxic Algal Blooms*; Yasumoto, T., Oshima, Y., Fukuyo, Y., Ed.; Intergovernmental Oceanographic Commission of UNESCO: Paris, 1996; pp 503−506.
(4) Paul, G. K.; Matsumori, N.; Konoki, K.; Murata, M.; Tachibana, K. *J. Mar. Biotechnol.* **1997**, *5*, 124–128.
(5) Murata, M.; Matsuoka, S.; Matsumori, N.; Paul, G. K.; Tachibana, K. *J. Am. Chem. Soc.* **1999**, *121*, 870–871.
(6) Morsy, N.; Matsuoka, S.; Houdai, T.; Matsumori, N.; Adachi, S.; Murata, M.; Iwashita, T.; Fujita, T. *Tetrahedron* **2005**, *61*, 8606–8610.
(7) Morsy, N.; Houdai, T.; Matsuoka, S.; Matsumori, N.; Adachi, S.; Oishi, T.; Murata, M.; Iwashita, T.; Fujita, T. *Bioorg. Med. Chem.* **2006**, *14*, 6548–6554.
(8) Doi, Y.; Ishibashi, M.; Nakamichi, H.; Kosaka, T.; Ishikawa, T.; Kobayashi, J. *J. Org. Chem.* **1997**, *62*, 3820–3823.
(9) Huang, X.-C.; Zhao, D.; Guo, Y.-W.; Wu, H.-M.; Trivellone, E. *Tetrahedron Lett.* **2004**, *45*, 5501–5504.
(10) Washida, K.; Koyama, T.; Yamda, K.; Kita, M.; Uemura, D. *Tetrahedron Lett.* **2006**, *47*, 2521–2525.
(11) Houdai, T.; Matsuoka, S.; Matsumori, N.; Murata, M. *Biochim. Biophys. Acta* **2004**, *14*, 5677–5680.
(12) Houdai, T.; Matsuoka, S.; Morsy, N.; Matsumori, N.; Satake, M.; Murata, M. *Tetrahedron* **2005**, *61*, 2795–2802.
(13) Morsy, N.; Houdai, T.; Konoki, K.; Matsumori, N.; Oishi, T.; Murata, M. *Bioorg. Med. Chem.* **2008**, *16*, 3084–3090.

10.1021/ol8016337 CCC: $40.75
Published on Web 09/04/2008

insight into the membrane-bound structure of AM, conformational analysis of AM3 was carried out using SDS micelles as a membrane model[12] and revealed that the central region of AM3 takes a hairpin conformation while the hydrophobic polyolefin region is immersed in the micelle interior.

However, use of SDS micelles as a membrane model often causes controversy because of the small radius of curvature, the lack of planar bilayer structures, and the different polar-head functionalities from those of phospholipids. Recently, it was shown that phospholipid bicelles provide a more natural membrane environment because of the presence of planar lipid bilayer portions.[14,15] Bicelles generally consist of long- and short-chain phospholipids, and their size depends on the ratio (q) of the long-chain phospholipids to the short-chain ones. At q values less than 2.5, bicelles adopt a disk-shaped morphology,[16−21] where the planar bilayer region formed by the long-chain lipid is surrounded by a rim consisting of the short-chain lipid. Unlike the large bicelles with $q > 2.5$ that are oriented parallel to the magnetic field, small bicelles with $q < 1$ are known to undergo fast tumbling in aqueous solutions while retaining the discoidal shape,[18−21] thus facilitating high-resolution NMR measurements of membrane-bound molecules. We have already used these isotropic small bicelles for determining the membrane-bound structure of erythromycin A, a widely prescribed macrolide antibiotic, and salinomycin, a well-known ionophore antibiotic, and demonstrated the general utility of isotropic bicelle media in determining the conformation and location of membrane-associated nonpeptidic molecules.[22,23] In the present study, we applied the isotropic bicelles to the conformation analysis of AM3 in a membrane environment. In addition, the topological orientation of AM3 within bicelles was also elucidated by monitoring the paramagnetic relaxation of proton signals in the presence of Mn^{2+}.

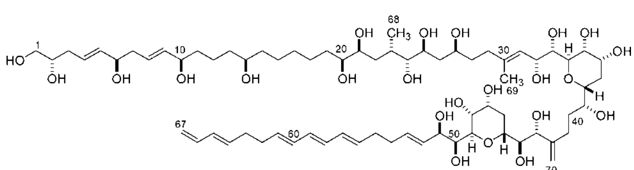

Amphidinol 3 (AM3)

In this study, we used typical isotropic bicelles composed of dimyristoylphosphatidylcholine (DMPC) and dihexanoylphosphatidylcholine (DHPC) at a ratio of 1:2 ($q = 0.5$). AM3 was incorporated into the isotropic bicelles at 25 mol % of total phospholipids. The total lipid concentration was set to 2.4% W/V in an aqueous solution. For measuring NMR spectra of AM3 in isotropic bicelles, we used deuterated phospholipids DMPC-d_{54} and DHPC-d_{22}, in which hydrogen atoms in acyl chains are replaced by deuteriums. A series of DQF-COSY, TOCSY, and NOESY spectra were utilized to fully assign the proton resonances (Table S1 in Supporting Information).

Then, we determined the conformation of AM3 associated with isotropic bicelles on the basis of the NOEs and $^3J_{HH}$ values obtained from the NOESY and DQF-COSY experiments, respectively. NOESY cross-peaks were categorized into three groups with upper distance limits of 3.0, 4.0, and 5.0 Å (Table S1, Supporting Information) according to NOE intensities. However, conformationally relevant NOEs were not observed for the C1−C20 or the polyene portion, and therefore conformation analysis was carried out for the C20−C54 portion of AM3. We also utilized $^3J_{HH}$ values to restrain the dihedral angles in the C31−C35, C43−C45, and C49−C50 bonds of AM3 (Table 1). Other $^3J_{HH}$ values were not obtained due to signal overlapping and low signal intensity in the DQF-COSY spectrum. The typical large and small values of the vicinal coupling constants, as listed in Table 1, indicate that rotational averaging rarely takes place for these bonds in major conformers except for the C38−C39 bond where no rotational constraint was applied due to the intermediate coupling value. The total numbers of interproton distances and dihedral restraints derived from the NMR data were 76 and 7, respectively. Since there were no NOEs between the C20−C54 and the other portions, it is unlikely that the conformation of the C20−C54 is affected by the other moieties. Upon calculation, we applied a continuum solvation model for water using a generalized Born-surface area (GB/SA) method,[24] because most of the AM3 molecule except for the polyene is likely in the water-accessible region of bicelles as estimated below. Under these conditions, 3000 random conformers were generated by using a systematic Monte Carlo conformation search algorithm,[25] and each

Table 1. $^3J_{HH}$ values of AM3 in Isotropic Bicelles[a]

coupled protons	$^3J_{HH}$ (Hz)	coupled protons	$^3J_{HH}$ (Hz)
H-31/H-32	8	H-43/H-44	9
H-32/H-33	<3	H-44/H-45	<3
H-33/H-34	10	H-49/H-50	10
H-38/H-39	7	H-50/H-51	<3

[a] Data were extracted from the DQF-COSY spectrum (see Supporting Information).

(14) Sanders, C. R.; Hare, B. J.; Howard, K. P.; Prestegard, J. H. *Prog. Nucl. Magn. Reson. Spectrosc.* **1994**, *26*, 421–444.
(15) Chou, J. J.; Kaufman, J. D.; Stahl, S. J.; Wingfield, P. T.; Bax, A. *J. Am. Chem. Soc.* **2002**, *124*, 2450–2451.
(16) Lin, T. L.; Liu, C. C.; Roberts, M. F.; Chen, S. H. *J. Phys. Chem.* **1991**, *95*, 6020–6027.
(17) Vold, R. R.; Prosser, R. S. *J. Magn. Reson., Ser. B* **1996**, *113*, 267–271.
(18) Glover, K. J.; Whiles, J. A.; Wu, G. H.; Yu, N. J.; Deems, R.; Struppe, J. O.; Stark, R. E.; Komives, E. A.; Vold, R. R. *Biophys. J.* **2001**, *81*, 2163–2171.
(19) Luchette, P. A.; Vetman, T. N.; Prosser, R. S.; Hancock, R. E. W.; Nieh, M. P.; Glinka, C. J.; Krueger, S.; Katsaras, J. *Biochim. Biophys. Acta* **2001**, *1513*, 83–94.
(20) van Dam, L.; Karlsson, G.; Edwards, K. *Biochim. Biophys. Acta* **2004**, *1664*, 241–256.
(21) Andersson, A.; Mäler, L. *Langmuir* **2006**, *22*, 2447−2449.
(22) Matsumori, N.; Morooka, A.; Murata, M. *J. Med. Chem.* **2006**, *49*, 3501–3508.
(23) Matsumori, N.; Morooka, A.; Murata, M. *J. Am. Chem. Soc.* **2007**, *129*, 14989–14995.
(24) Still, W. C.; Tempczyk, A.; Hawley, R. C.; Hendrickson, T. *J. Am. Chem. Soc.* **1990**, *112*, 6127–6129.

conformer was subjected to energy minimization by the conjugate gradient method using the MMFF force field.[26] Figure 1 shows the lowest-energy conformations of the

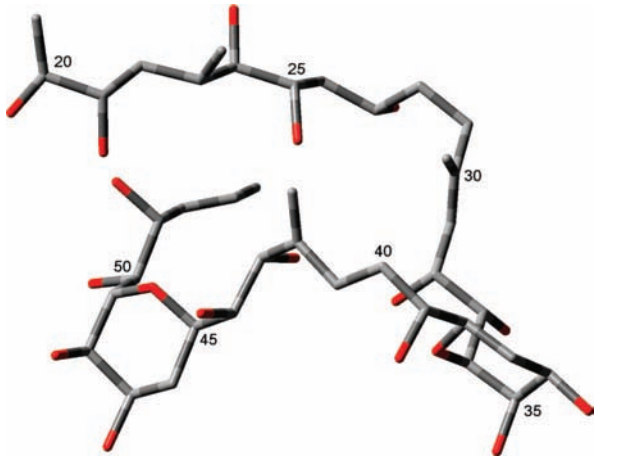

Figure 1. Lowest-energy conformation for the C20−C54 portion of AM3 in isotropic bicelles ($q = 0.5$). The second lowest-energy conformation is unstable by 1.5 kcal/mol. Calculation was performed with a systematic Monte Carlo method constrained by NOE and $^3J_{HH}$ data. Hydrogen atoms are omitted for clarity.

C20−C54 portion AM3 in isotropic bicelles. The second lowest-energy conformation is energetically unstable by 1.5 kcal/mol, whose contribution can be neglected because its population is estimated to be less than 1/10. Therefore, we focused on the lowest-energy conformation. As can be seen in this figure, AM3 appears to have turn structures at the two tetrahydropyran rings.

Paramagnetic agents enhance the relaxation of NMR nuclei in their vicinity, and the relaxation induced by Mn^{2+} has been frequently used to estimate molecular segments that are exposed to the aqueous exterior of membranes. The paramagnetic contribution to spin−lattice relaxation is represented by T_{1M}

$$T_{1M} = T_{1P} \cdot T_1^0/(T_1^0 - T_{1P})$$

where T_1^0 and T_{1P} are the spin−lattice relaxation times in the absence and presence of the paramagnetic agent, respectively.[27] The paramagnetic relaxation time T_{1M} has explicit r^6 distance dependency, thus making it possible to evaluate semiquantitatively the depth of membrane-bound entities.

We measured the T_{1M} values of AM3 protons in bicelles containing Mn^{2+} (Figure 2), though only a limited number of T_{1M} values were available because of overlapping signals on one-dimensional NMR. As shown in Figure 2, H-66 and H-67, the terminal protons, have larger T_{1M} values because they are less affected by Mn^{2+}, suggesting the deeper immersion of the terminal diene into the hydrophobic region.

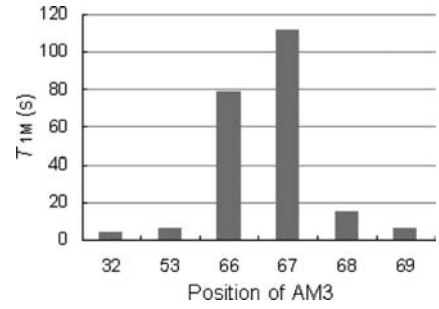

Figure 2. Effects of Mn^{2+} on proton relaxation times of AM3 in isotropic bicelles. The figure depicts the T_{1M} (s) in the presence of 10 μM Mn^{2+}. Larger T_{1M} values are indicative of longer distances from the membrane surface.

Meanwhile, other protons in Figure 2 are significantly affected by Mn^{2+} as is clear from smaller T_{1M} values, indicating the distribution in the membrane/water interface.

On the basis of current findings using isotropic bicelles, we propose a model of structure and position of AM3 in membranes (Figure 3). The deeper immersion of the terminal

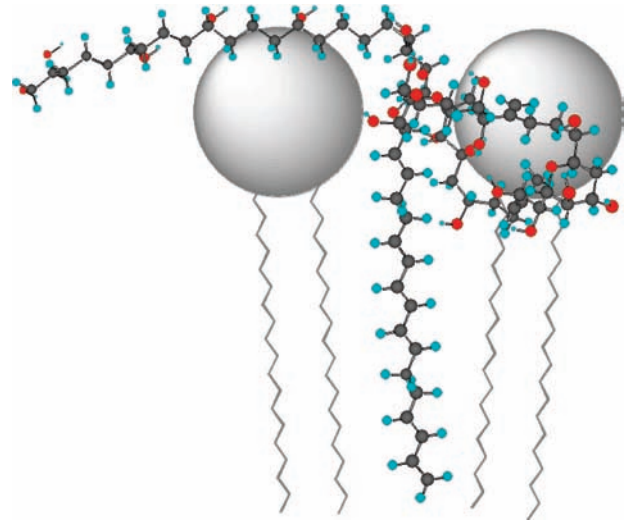

Figure 3. Hypothetical model of the membrane-bound structure of AM3.

diene into the membrane interior, as revealed by the Mn^{2+} relaxation experiment, suggests the predominance of extended conformation for the hydrophobic polyene portion. Although the conformation of C1−C20 remains unelucidated due to the high flexibility, AM3 is likely to take an umbrella-like or a T-shaped structure in the membrane, comprised of a bent polyol portion with a large cross-section area and the extended polyene chain with a smaller cross-section.

We reported that AM3 in SDS micelles takes a hairpin conformation in the central region (C20−C52 moiety). The hydrophilic region of AM3 is predominantly present in the surface, while the hydrophobic polyolefin region penetrates

(25) Goodman, J. M.; Still, W. C. *J. Comput. Chem.* **1991**, *12*, 1110–1117.
(26) Halgren, T. A. *J. Comput. Chem.* **1996**, *17*, 490−512, 520−552, 553−586, 587−615, 616−641.
(27) Villalaín, J. *Eur. J. Biochem.* **1996**, *241*, 583–593.

in the interior of SDS micelles.[12] Accordingly, the conformation and position of AM3 turn out to be less variable in SDS micelles and in bicelles, which suggests that the structural and positional preference of AM3 is essentially unaffected by media used. In addition, the polyol portion of AM3 was shown to reside in a hydrophilic water-accessible region, where hydrogen bonding is weakened in comparison with that in the hydrophobic environment. Therefore, we consider that hydrogen bonding does not play a major role in regulating the conformation of AM3 in membrane environments.

Recently, we observed that AM-induced membrane permeabilization is hardly influenced by membrane hydrocarbon thickness.[13] This findings support the toroidal pore formation by AM3 rather than the barrel-stave pore because the stability of the barrel-stave pore generally depends on the membrane thickness; the hydrophobic mismatch between the length of the transmembrane domain of the pore and the bilayer hydrocarbon region hampers formation of the barrel-stave assembly.[28] On the other hand, the toroidal pore-formers are always associated with the lipid headgroups even when they are perpendicularly inserted in the lipid bilayer. In such a pore, the lipid monolayer curves continuously from the outer leaflet to the inner in the fashion of a toroidal hole, so that the pore is lined by both the pore-formers and the lipid headgroups. From this viewpoint, the structure of AM3 shown in Figure 3 seems suitable for toroidal pore formation: (1) the disproportionally large hydrophilic portion of AM3 as compared with the hydrophobic polyene chain can induce a positive curvature strain to the membrane surface, (2) the long and hairpin-shaped polyhydroxy chain of AM3 is likely to effectively capture the polar headgroups of lipids, and (3) the resultant association between the hydrophilic chain of AM3 and the lipid head groups may be able to form the inner lining of the toroidal pore. The high curvature of the AM3-bound membrane is evidenced by our previous finding that AM3 takes a similar hairpin conformation and is immersed to a similar extent in SDS micelles where the small globular shape induces intrinsic curvature.

In conclusion we have determined the structure and location of AM3 in a membrane environment using isotropic bicelles. The results show that AM3 takes turn structures at the two tetrahydropyran rings. Most of the hydrophilic region of the molecule is predominantly present in the surface, while the hydrophobic polyolefin penetrates in the bicelle interior. This conformational and positional preference of AM3 is considered to play a crucial role for toroidal pore formation in biological membranes. In addition, this study demonstrates the general applicability of the bicelle system to conformational analyses of membrane-bound natural products with molecular weights larger than 1000 Da.

In the previous report,[13] we have shown that cholesterol potentiates the membrane-permeabilizing activity of AM3 even at 0.5% (wt/wt) to the lipid, which ruled out the possibility that alteration of the membrane physical properties induced by cholesterol was chiefly responsible for this cholesterol effect. This suggests that cholesterol directly interacts with AM3 and is involved in the pore complex. The detailed evaluation of the interaction between AM3 and cholesterol is now in progress using the bicelle system and other methods.

Acknowledgment. We are grateful to Mr. Seiji Adachi in our department for his assistance in NMR measurements. This work was supported by Grant-In-Aids for Scientific Research (A) (No.15201048) and (S) (No. 18101010), for Priority Area (A) (No. 16073211), and for Young Scientists (A) (No. 17681027) from MEXT, Japan, and by a grant from the CREST, Japan Science and Technology Corporation.

Supporting Information Available: Experimental details, table of ^{1}H NMR chemical shifts and NOE data, and NMR spectra of AM3 in bicelles. This material is available free of charge via the Internet at http://pubs.acs.org.

OL8016337

(28) Allende, D.; Simon, S. A.; McIntosh, T. J. *Biophys. J.* **2005**, *88*, 1828–1837.